

# Robust Power Control and Task Offloading for Cloud Assisted MEC in Vehicular Networks

Zhixin Liu, *Senior Member, IEEE*, Jianshuai Wei, Jiawei Su, Kit Yan Chan, Yazhou Yuan, and Xinping Guan,  
*Fellow, IEEE*

**Abstract**—Cloud-assisted mobile-edge computing (C-MEC) is been witnessed as a novel solution for task offloading in vehicular networks, which is able to provide rich computing resources. In this paper, a robust power control and task offloading scheme is proposed to offload the computation task and maximize the utility of C-MEC networks. However, an uncertain channel state influences the stability of transmitting the offloading task significantly. In order to simulate channel uncertainty, a first-order Markov process has been adopted, where the vehicular mobility is considered. Moreover, channel reusing is assumed to be caused by the limited spectrum resources and which leads to complex co-channel interference is generated. To overcome the limitations, probability constraints of signal links are enforced to ensure communication quality. A Bernstein approximations method is adopted to transform the original constraints into solvable constraints. Scrupulously, the block coordinate descent (BCD) method and the successive convex approximation (SCA) technique are further adopted to solve the nonconvex robust optimization problem. A robust power control and task offloading scheduling algorithm is proposed to determine the optimal solutions. The proposed algorithm has been subjected to numerical simulations in order to assess the system's performance. The results obtained have demonstrated its effectiveness over the benchmark models, especially in communication environments with channel uncertainty.

**Index Terms**—Internet of Vehicle (IoV), Computation Offloading, Robust Power Control, Edge Computing, Bernstein Method,

## I. INTRODUCTION

Mobile-edge computing (MEC) and mobile cloud computing (MCC), as two new architectures for the emerging 5G networks, are commonly used to support task offloading for Internet of Things devices, especially providing the low-latency and high-reliability computing services [1], [2]. At the edge of the network center, MEC reduces transmission delay and allocates computing resources to vehicles to relieve the computational pressures [3]. However, the computational resources of MEC are still inadequately when the computational tasks are demanding. Since the high performance computing

is provided by cloud servers, cloud-based computing networks have been deployed to satisfy explosive-growth demands of computation offloading. However, cloud computing centers tend to be far from the road. In the high-dynamic Internet of Vehicles, the data transmitted by vehicles must be processed in a real time [4]. Therefore, the C-MEC is deployed for the network architecture, in order to provide rich computing resources and reduce transmission latency.

However, interference in the dynamic vehicle scenario often result in a significantly deteriorated communication Quality of Service (QoS) to the current Mobile-Edge computing that enables vehicular networks. In addition, vehicle mobility causes an uncertain channel state and it further significantly impact and destabilize communication quality. Deploying joint power control and computing resource allocation in the multi-vehicles in multi-MEC systems will resolve the task offloading problem in a C-MEC vehicular network and will guarantee the QoS.

### A. Related Works

Recently, some research has been conducted to improve the effectiveness and robustness of IoV edge computing networks, which consist of a cloud computing layers and MEC layer vehicle network architectures. Zhou et al. [5] proposed a computing framework for vehicular networks with a hierarchical structure, which is composed of the control layer, the vehicular edge computing server layer, and the vehicular network layer. Dai et al. [6] conducted researched on enhancing the cooperative computation offloading service in MEC-assisted service architecture, where the multiple MEC servers and remote cloud offloading of computation-intensive tasks are implemented in a collaborative way. Some research proposed methods to improve computation offloading performance in the C-MEC vehicular network scenario. Tan and Hu [7] have formulated and solved the joint communication, caching, and computing problem, in order to optimize the operational excellence and cost efficiency of vehicular networks. Wang et al. [3] formulated the problem as a generalized NE problem and proposed a game theory algorithm to analyze the equilibrium problem. Wang et al. [8] developed a distributed clustering mechanism which organizes vehicles into several cooperative edge servers to optimize the total revenue during the entire scheduling process. Li et al. [9] developed an analytical model of the service cache at the edge of the vehicle, mainly considering the computational task offloading and task interdependence between RSUs. However, the aforementioned

Zhixin Liu, Jianshuai Wei, Jiawei Su and Yazhou Yuan are with the School of Electrical Engineering, Yanshan University, Qinhuangdao 066004, China. Emails: lzxauto@ysu.edu.cn, jswe@stumail.ysu.edu.cn, sjw@stumail.ysu.edu.cn, yzyuan@ysu.edu.cn.

Kit Yan Chan is with the School of Electrical Engineering, Computing and Mathematical Sciences, Curtin University, Perth, Australia. Email: k-it.chan@curtin.edu.au.

Xinping Guan is with the School of Electronic, Information and Electrical Engineering, Shanghai Jiaotong University, Shanghai 200240, China. Email: xpguan@sjtu.edu.cn.

This work is supported partly by National Natural Science Foundation of China under Grant 62273298, 62273295.

methods only optimized one of the two indexes, power control and computing resource allocation. Some research assumed that the vehicles maintain a constant transmit power, our approach takes a multi-faceted approach towards optimization which includes optimizing both the vehicle's transmit power and the computational resource allocation for a multi-vehicles and multi-MEC servers system. A new challenge is created since the objective function is difficult to optimize. A convex approximation approach for optimizing the objective function has been suggested by Nemirovski and Shapiro. [10]. To solve the non-convex problems with two variables, some research decouples the original problem into two subproblems and the BCD method is employed to address the two subproblems.

Unlike the traditional mobile communications networks with low mobility, the Doppler effect in the high mobility of vehicles poses a challenge to C-MEC communication, when the fast-moving vehicles communicate with different MEC servers. The deterministic channel state information (CSI) is no longer sufficient to describe the channel state in network scenarios with dynamic characteristics. The Doppler effect created during transmission significantly impacts the small-scale fading of CSI, resulting in fast channel variations. In other words, the used CSIs are obsolete. To depict the effects of Doppler frequency shift on the channel, the First-order Gauss-Markov process is utilized [11]. In order to improve the performance with low communication delay and computing delays, vehicle equipment has a reduced delay tolerance and transmission reliability. Therefore, higher requirements are essential. In [12], Li et al. in order to ensure the reliability of vehicular communication links, an outage probability constraint is introduced. When the exact expression exists the exponential integral function, it is necessary to consider an approximate closed-form expression to make it tractable so as to reduce the computational complexity.

In C-MEC vehicular networks, authorized vehicles with spectrum resources directly communicate with RSU. However, scarce spectrum resources is inadequate in high-density vehicular networks [13]. Zhou et al. [14] developed a dynamic sharing approach for 5G spectrums and they proposed a sharing architecture of DSRC and the 5G spectrum to enable immersive experience-driven vehicular communications. Tran et al. [15] proposed a comprehensive approach to tackle the challenge of task offloading and resource allocation in a multi-server MEC-assisted network. The results showed that effective channel reusing is crucial when the spectrum resources are scarce [16]. However, the approach generally creates interference, where the interference caused by channel reuse in the vehicle communication scenario often degrades acutely the communication quality. To simulate the interference constraint, the probability constraints are introduced to resolve the uncertain co-channel interference, and the Bernstein approximation method is used to transform the interference constraint into a solvable closed form. The method has commonly been used to solve the hard non-convex problems [17]. To deal with the outage probability constraint, Xiao et al. [18] assumed the CSIs are can be obtained by estimation. Therefore, the outage constraint is transformed as the Bernstein-type inequality, in order to formulate the deterministic optimization problem [19].

Additionally, the paper employs the Bernstein method because of the uncertain constraint characteristics. In summary, existing research has tackled power control and computing resource allocation problems in cloud which assists MEC in vehicular networks in high dynamic environments; also no research attempts to ensure communication quality and latency requirements are satisfactory.

## B. Contributions

In this paper, a robust power control and task offloading algorithm is proposed for the cloud, in order to assist MEC in vehicular networks with highly dynamic vehicles. Unlike the existing unilateral research on power control or resource allocation computation, a network system that heavily emphasizes collaboration is investigated and the communication delay and computing delay are guaranteed by satisfying the probabilistic constraints; vehicle QoS is also guaranteed in the framework. To summarize, this paper's primary contributions can be outlined as follows:

- We present a C-MEC vehicular networks for computation offloading architecture. Since the MEC layer is deployed close to the networks and has computation capacity, the MEC layer can serve as a bridge between vehicles and the cloud server. The cloud computing layer process delay-insensitive and large-scale data which the MEC layer cannot process. This network architecture reduces transmission time and provides large computing resource.
- A first-order Markov process has been adopted to resolve the channel uncertainty caused by the high-speed movement of vehicles. A feasible IoV network scenario is constructed to simulate the dynamic characteristics of the C-MEC vehicular networks. The Bernstein method is used to approximate non-convex outage constraint for large-scale dynamic in vehicle network environments.
- We propose an efficient hybrid strategy to schedule transmission tasks. V2R transmission is utilized to reduce delays when a task-initiating vehicle is unable to complete a task independently under C-MEC vehicular networks.

The rest of this paper is organized as follows: the model of power control and task offloading for cloud assisted MEC in vehicular networks is presented in Section II. In Section III, the objective function and the non-convex constraints are formulated, and the problem solutions are proposed. In Section IV, the performance evaluations are presented. Finally, we conclude the paper in Section V.

## II. SYSTEM MODEL

In this research, the C-MEC vehicular network is shown in Fig. 1, which is composed of the MEC layer and the cloud computing layer hierarchical architecture of computational offloading. Numerous vehicles are divided into multiple geographic zones within the RSUs coverage underlay a cell, and each RSU is equipped with a MEC server to provide computation offloading services to the vehicles. We denote two sets of vehicles and MEC servers in the mobile system as  $\mathcal{V} = \{1, 2, \dots, V\}$  and  $\mathcal{M} = \{1, 2, \dots, M\}$ , respectively. The

high-speed mobile wireless communication link is denoted as V2RSU (V2R) link, and the fixed wired connection link is denoted as RSU to Cloud (R2C) link. The detailed offloading process is described as follows. Firstly, the vehicles offload request messages by the wireless interface, which includes the required communication resources, the task ID and submission time, and the maximum tolerable service times of the task to the cloud. Second, the MEC server performs scheduling according to the received request messages, including the task upload server and task computation server. Finally, after the task is uploaded, the task is pushed in the server queue until the server execute the task. Furthermore, some notations used in this paper are given in Table I.

**Remark 1.** In this article, we consider only simplified cases within one time slot to arrive at a tractable solution. Nevertheless, by utilizing time division multiple access communication technology, the proposed solution can be readily expanded to accommodate a multi-segment scenario. The vehicles in each RSU coverage communication are divided into different collections. Hence, time resource is divided into multi-frames, and each frame is divided into several time slots. Different vehicles access its time slots when they communicate with the RSU.

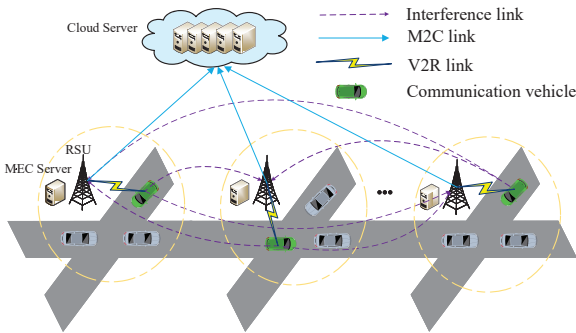


Fig. 1: System model.

TABLE I: Notations

|                |  |
|----------------|--|
| $\Pr\{\cdot\}$ | Probability function.  |
| $\mathbb{R}^k$ | Set of $k$ -dimensional real vectors.  |
| $\mathbf{f}$   | Index set of computing resource $\mathbf{f}=[f_1, \dots, f_i, \dots, f_M]$ . |
| $\mathbf{p}$   | Index set of vehicle power $\mathbf{p}=[p_1, \dots, p_i, \dots, p_M]$ .      |
| $\mathcal{M}$  | Index set of vehicles over a time slot $\mathcal{M}=\{1, 2, \dots, M\}$ .    |
| $\mathcal{V}$  | Index set of all active vehicles $\mathcal{V}=\{1, 2, \dots, V\}$ .          |
| $E\{\cdot\}$   | Expected value of a random variable.   |

#### A. Communication Model

Since the vehicle mobility is fast, the communication model is different to traditional cellular communications. Hence, the CSI is hard to be obtained directly. In particular, RSU only obtains accurate knowledge of large-scale fading  $L^2$  of vehicular to RSU links while the small-scale fading  $h$  is greatly influenced by the fast channel variations caused by the Doppler effect. We assume the CSIs are obtained through channel

estimation [18]. Therefore, we model the small-scale fading channel estimation of  $h$  by using the first-order Gauss-Markov process [20] in each transmission time interval as follows,

$$h = \xi \tilde{h} + \sqrt{1 - \xi^2} \zeta. \quad (1)$$

we assume that the estimated channel gain  $\tilde{h}$  denotes the estimate of  $h$  and  $\tilde{h}^2$  is exponentially distributed with the unit mean [21]. Furthermore,  $\xi \in (0, 1)$  represents the correlation coefficient over V2R link, and  $\zeta$  denotes the channel gain with a Complex Gaussian distribution  $\zeta \sim CN(0, \delta^2)$  which is independent and uncorrelated of  $\tilde{h}$ . The coefficient ( $0 < \zeta < 1$ ) quantifies the channel correlation between two consecutive time slots and we assume that the same time correlation coefficient  $\zeta$  exists for all vehicles. Jakes statistical model for the fading channel [20], states that  $\zeta = J_0(2\pi f_{max} T_s)$ , where  $J_0$  is the zero-order Bessel function of the first kind.  $f_{max} = \bar{v} f_c / c$  is the maximum Doppler frequency, where  $\bar{v}$  denotes the vehicle speed,  $f_c$  denotes the carrier frequency at 5.9 GHz, and  $c = 3 \times 10^8$  m/s,  $T_s$  is a period feedback latency. Both transmitter vehicles and RSU know the actual  $\zeta$ .

Based on the aforementioned discussion, the mobile V2R channel power gain of the effective links and interference links at the  $k$ th time slot from the  $i$ th vehicle transmitter to the  $j$ th receiver is expressed as a shared expression:

$$G_{i,j}^k = \tilde{g}_{i,j}^k + \hat{g}_{i,j}^k, \quad (2)$$

where  $\tilde{g}_{i,j}^k = L_{i,j}^2 \tilde{h}_{i,j}^2 \xi_{i,j}^2$ ,  $\hat{g}_{i,j}^k = L_{i,j}^2 (1 - \xi_{i,j}^2) \zeta_{i,j}^2$ , and  $L_{i,j}^2$  denotes large-scale fading effects at the  $k$ th time slot including shadow-fading and path loss from the  $i$ th vehicle transmitter to the  $j$ th receiver on the road. Moreover,  $\hat{g}_{i,j}^k$  is an observed value and  $\tilde{g}_{i,j}^k$  expresses an exponential random variable with the parameter  $\frac{1}{L_{i,j}^2 (1 - \xi_{i,j}^2)}$  which is based on [13].

To improve the spectrum utilization and realize multi-vehicles joint communication, V2R communications reuse the same uplink channel. In this case, the Signal-to-Interference-plus-Noise Ratio (SINR) of V2R link is formulated as,

$$\gamma_i(\mathbf{p}) = \frac{p_i g_{i,i}}{\sum_{j=1, j \neq i}^M p_j g_{j,i} + \sigma^2}, \quad (3)$$

where  $p_j$  denotes the transmit power of the  $j$ th vehicles, and  $\sigma^2$  is the background noise. Therefore, the deterministic equivalent transmission rate of vehicles is calculated by Shannons theorem as,

$$R_i(\mathbf{p}) = \log_2 \left( 1 + \frac{p_i g_{i,i}}{\sum_{j=1, j \neq i}^M p_j g_{j,i} + \sigma^2} \right). \quad (4)$$

The transmission time of vehicle  $i$  is defined as  $t_{i,up}$  when sending its task input to the uplink when input parameters are denoted  $d_{i,up}$  can be calculated as,

$$t_{i,up} = \frac{d_{i,up}}{R_i(\mathbf{p})}, \quad (5)$$

Therefore, the upload time of each V2R link is formulated as,

$$t_{i,up} = \frac{d_{i,up}}{W \log_2 \left( 1 + \frac{p_i g_{i,i}}{\sum_{j=1, j \neq i}^M p_j g_{j,i} + \sigma^2} \right)}, \quad (6)$$

Here,  $W$  represents the bandwidth of the reused channel by multiple V2R links, and  $d_{i,up}$  is the size of input data including system settings, program codes, and input parameters, which are necessary to be transmitted for the program execution.

The communication delay is another significant factor that impacts the performance of vehicular networks. The packets to RSUs must be in the queue before the transmission, where the transmission speed is  $R_i$ . The packet arrival process at the  $i$ th V2R receiver follows a Poisson process with parameter  $k_i$ , and the length of the data packet is exponentially distributed with parameter  $\tau_i$ . Since  $M/M/1$  queueing based method can guarantee the vehicular communications reliability [22], we utilize the  $M/M/1$  model to analyze the system and express the expected delay as a function of the transmission rate of the  $i$ th V2R link is expressed as,

$$D_i = \frac{1}{\tau_i R_i - k_i}. \quad (7)$$

### B. Vehicle Computing Model

We denote the number of CPU cycles required to process 1-bit of input data at vehicle  $i$  as  $c_0$  [23], which is indivisible and cannot be broken down into smaller components [24]. We consider that each vehicle  $v \in \mathcal{V}$  has a different computational task at a time, denoted as  $T_i$ , is defined by a tuple consisting of two parameters,  $\langle d_{i,up}, c_{i,e} \rangle$ , in which  $c_{i,e}$  [cycles] specifies the workload [15]. Hence, the computation cost to accomplish the task,  $c_{i,e}$  can be obtained through  $c_0 * d_{i,up}$  [25]. Each task is offloaded to the MEC server and then transmit to the cloud servers. By offloading the computation task to the MEC servers, the vehicles have more computing resources. However, additional time is likely to be consumed for transmitting the task input in the uplink direction.

The MEC server at each RSU provides the computational offloading service to a vehicle at a time slot. The computational resources are quantified by the fixed rate  $\bar{f}$ , which is the number of CPU cycles per second. The  $i$ th vehicle uploads the input data of each task to the nearest RSU. The RSU process the small-scale, delay-sensitive data first, and then the RSU forward the remaining data to the remote cloud server. The cloud server provides computation service to multiple RSUs at the same time. The computational resources available to RSUs are determined by the computational rate  $f_i$  allocated from the cloud servers, which is the number of CPU cycles per second. Therefore, the latency caused by the computational offloading can be computed as,

$$t_{i,exe} = \frac{c_{i,e}}{\bar{f} + f_i}. \quad (8)$$

### C. Problem Definition

Given that the computational rate  $f_i$ , the total delay experienced by vehicle  $i$  caused by offloading is given by,

$$t_i = \frac{c_{i,e}}{\bar{f} + f_i} + T_c, \quad (9)$$

where the transmission latency between cloud server and RSU is defined as  $T_c$ , which is usually set as a constant value [18].

Therefore the relative utility function in task completion time is characterized by,

$$U_{i,exe} = \frac{t_{max} - t_{i,exe}}{t_{max}}, \quad (10)$$

where  $t_{max}$  is the maximum time of the task completion tolerable threshold. If a task is completed within  $t_{max}$ , the vehicle has a higher utility. Otherwise, it produces the corresponding loss. Therefore, the utility of vehicle  $i$  for offloading is defined as  $\frac{U_{i,exe}}{t_{i,up}}$ , which is the offloading utility function per unit of time.

The power control and task offloading is formulated as an optimization problem in this section, which attempts to minimize the total system cost composed of latency and transmission rate for all vehicles in the networks. Given the uplink power allocation vector  $\mathbf{p}$  and the computational rate vector  $\mathbf{f}$ , the system utility is defined as the weighted sum of the unloading utility of all vehicles,

$$U = \sum_{i=1}^M \frac{U_{i,exe}}{t_{i,up}}, \quad (11)$$

where  $U$  is a more enormous execution time utility with a minor upload time cost. We formulate the robust optimization problem namely Power Control and Task Offloading Problem as a system utility maximization problem,

$$\max_{\mathbf{p}, \mathbf{f}} \sum_{i=1}^M \frac{U_{i,exe}}{t_{i,up}} \quad (12a)$$

$$\text{s.t.} \begin{cases} \Pr \{ \gamma_i \geq \gamma_{th} \} \geq 1 - \varepsilon_1, & (12b) \\ \Pr \left\{ \frac{1}{\tau_i R_i - k_i} + \frac{c_{i,e}}{\bar{f} + f_i} \leq D_{max} \right\} \geq 1 - \varepsilon_2, & (12c) \end{cases}$$

$$\sum_{i=1}^N f_i \leq f_{total}, \quad (12d)$$

$$0 \leq p_i \leq p_{max}, \quad (12e)$$

where  $U$  denotes the network utility. The constraints in (12) are explained as follows: Constraints (12b) guarantees the QoS requirements of vehicles. However, large amount of computation is caused by time varying network topologies. The real-time SINR is difficult to be quantified to obtain in vehicular communication scenario. The real time SINR is replaced with the long-term SINR since the CSI feedback time interval is very small. We use  $\gamma_i$  to represent the average SINR of the  $i$ th V2R link using a small CSI feedback time interval. To ensure that the task is successfully offloaded to the RSU, the SINR has to be larger than the SINR threshold [26].  $\gamma_{th}$  is the SINR threshold for detecting the V2R links communication.  $\Pr \{ \cdot \}$  defines the probability of the input SINR. The outage probability constraint (12b) guarantees the reliability of vehicular links [12].  $D_{max}$  represents the maximum allowable delay for the  $i$ th V2R link during the transmission of data. Additionally,  $\varepsilon_1$  and  $\varepsilon_2$  are the thresholds for the outage probabilities associated with the SINR and delay constraints, respectively, where  $\varepsilon_1, \varepsilon_2 \in (0, 1)$ . Constraint (12c) denote the total latency of communication and computation is larger than the delay threshold. Constraint (12d) ensures that cloud server has to allocate a computational resource to RSUs

associated with it and also constraint (12d) ensures that the total computational resources allocated to all the associated RSUs must not exceed the cloud server's computing capacity. Therefore, the number of applications served by a particular edge cloud has to be under its capacity. In constraint (12e),  $p_{max}$  is the maximum transmit power of the transmit vehicle in the vehicle communication network, and the transmit power is greater than zero.

### III. PROBLEM SOLUTIONS

In this section, we proposed a BCD-based algorithm to solve the optimization problem (12). The BCD method decomposes the complex original problem to be decomposed into a succession of simpler subproblems [27]. The BCD method first divides, all variables are divided into two blocks and optimized alternatively.

To solve the problem (12), the problem can be optimized by fixing the optimization variables of the computational rate vector  $\mathbf{f}$ . The problem is tackled through alternating optimization of the two sub-problems. By removing the vector  $\mathbf{f}$ , the problem (12a) can be transformed into the following problem.

$$\mathbf{P1} : \max_{\mathbf{p}} \sum_{i=1}^M \frac{U_{i,exe}}{t_{i,up}} \quad (13a)$$

$$s.t. \begin{cases} \Pr\{\gamma_i \geq \gamma_{th}\} \geq 1 - \varepsilon_1, \\ \Pr\left\{\frac{1}{\tau_i R_i - k_i} + \frac{c_{i,e}}{f + f_i} \leq D_{max}\right\} \geq 1 - \varepsilon_2, \\ 0 \leq p_i \leq p_{max}. \end{cases} \quad (13b) \quad (13c) \quad (13d)$$

#### A. Successive Convex Approximation of the Objective Function

Since (13) is a non-convex and NP-hard since the objective function (13a) is in a logarithmic form because of the form of Shannons theorem in  $t_{i,up}$ . Here the SCA method is used to simplify problem (13a) as a solvable problem. The nether constraint is used to approximate the original function as follows,

$$\alpha \ln(z) + \beta \leq \ln(1+z), \quad (14)$$

where  $\alpha = \frac{z_0}{1+z_0}$  and  $\beta = \ln(1+z_0) - \frac{z_0}{1+z_0} \ln(z_0)$ . Each term in (14) can be transformed as  $A_k \ln(\gamma_k(e^{\tilde{p}})) + B_k$  by successive convex approximation, where  $A_k$  and  $B_k$  are chosen as  $A_k = \gamma_i / (1 + \gamma_i)$  and  $B_k = \ln(1 + \gamma_i) - A_k \ln(\gamma_i)$  with  $A_k=1$  and  $B_k=0$ . Each term of objective function can be written as follows,

$$\frac{1}{\ln 2} \sum_{i=1}^M \frac{U_{i,exe}}{d_{i,up}} [A_k \ln(\gamma(p)) + B_k], \quad (15)$$

Since the objective function in (13a) is in a fractional form of SINR, this is not easy to calculate directly. Hence, we use the variable substitution, i.e.  $\hat{p}_i = \ln p_i$ ,  $p_i = e^{\hat{p}_i}$ , and  $\hat{p}_i \leq \ln p_{max}$ ,  $\forall 1 \leq i \leq M$

$$U = \max \frac{1}{\ln 2} \sum_{i=1}^M \frac{U_{i,exe}}{d_{i,up}} [A_k \ln(\gamma(e^{\tilde{p}})) + B_k]. \quad (16)$$

#### B. Approximate of the Outage Probability Constraint

Since (13b) is uncertain and the objective function (13a) is a non-convex problem, optimizing (13) is difficult. It is necessary to design an algorithm with lower complexity to solve (13b). To formulate the uncertain channel gain, the statistical constraint is adopted to describe the uncertainty (13b) by considering the fast fading. To further simplify (13b), a matrix form is introduced. The general form of the channel gain is described as,

$$\Pr\{(\mathbf{G}_m)^T e^{\tilde{p}} + \sigma^2 \leq 0\} \geq 1 - \varepsilon_1, \quad (17)$$

where  $\mathbf{G}_m = [G_{1,m}, G_{2,m}, \dots, -\frac{G_{m,m}}{\gamma_{th}}, \dots, G_{M,m}]^T$ . Furthermore, the Bernstein method is adopted to approximate the probability constraint with channel uncertainty.

**Theorem 1.** *The outage probability of all V2R links represented as  $\Pr\{\gamma_i \geq \gamma_{th}\} \geq 1 - \varepsilon_1$  can be reformulated as separable constraints,*

$$\sigma^2 + \sum_{i \neq j}^M \chi_{i,j} e^{\tilde{p}_i} + \sqrt{2 \ln\left(\frac{1}{\varepsilon_1}\right)} \left( \sum_{i \neq j}^M (\sigma_{i,j} \beta_{i,j} p_i)^2 \right)^{\frac{1}{2}} \leq 0, \quad (18)$$

where  $\chi_{i,j} = \mu_{i,j}^+ \alpha_{i,j} + \beta_{i,j} + g_{i,j}$ . The parameters (i.e.,  $\sigma_{i,j}$  and  $\alpha_{i,j}$ ), are deduced to be positive in [11]. Suppose that the truncated distributions of  $G_{i,j}$  have the bounded ranges  $[\tilde{g}_{i,j}^k + \alpha_{i,j}, \tilde{g}_{i,j}^k + \beta_{i,j}]$ ,  $\tilde{g}_{i,j}^k$  is an estimate of  $G_{i,j}$ . The constants  $\alpha_{i,j} = \frac{1}{2}(b_{i,j} - a_{i,j})$ ,  $\beta_{i,j} = \frac{1}{2}(b_{i,j} + a_{i,j})$  are used to normalize the ranges to  $[-1, 1]$  as follows,

$$\xi_{i,j} = \frac{G_{i,j} - \tilde{g}_{i,j}^k - \beta_{i,j}}{\alpha_{i,j}} \in [-1, 1]. \quad (19)$$

In the last term of (18), the variables  $p_i$  are coupled nonlinearly. Hence, determining an acceptable good solution to (13b) is time consuming by the Bernstein method when  $k$  increases and the number of vehicles is large. Therefore, it is necessary to introduce a  $\ell_2$ -norm approximate problem for any  $\mathbf{x} \in \mathbb{R}^k$ . Hence, the last term in (18) containing the  $\ell_2$ -norm of the vector  $\mathbf{x} = [\sigma_{i,1} \beta_{i,1} p_i, \dots, \sigma_{i,M} \beta_{i,M} p_i]$  is further approximated by  $\|\mathbf{x}\|_2 \leq \|\mathbf{x}\|_1$ . The constraint in (13a) is further formulated as (20), where the complexity is reduced and the reliability is improved.

$$\sigma^2 + \sum_{i \neq j}^M \chi_{i,j} e^{\tilde{p}_i} + \sqrt{2 \ln\left(\frac{1}{\varepsilon_1}\right)} \sum_{i \neq j}^M |\sigma_{i,j} \beta_{i,j}| e^{\tilde{p}_i} \leq 0, \quad (20)$$

To pursue a simple form of (20), we define

$$\Pi_i = \sigma^2 + \sqrt{2 \ln\left(\frac{1}{\varepsilon_1}\right)} \sum_{i \neq j}^M |\sigma_{i,j} \beta_{i,j}| e^{\tilde{p}_i}. \quad (21)$$

Constraint (13c) is reformulated by an Integral transformation method. According to constraint (13c),  $X = \tilde{h}^2$  is an exponential random variable with unit mean, i.e.  $X \sim \exp(1)$ , where  $D_{max} = D_1 + D_2$ ,  $D_1 = \frac{1}{\tau_i R_i - k_i}$ , and  $D_2 = \frac{c_{i,e}}{f_i}$ . We can determine the feasible power region of the communication delay probability as follows,

$$[\ln(1 - \varepsilon_2) - \hat{g}_{i,j}^k] e^{\tilde{p}_i} + D^* \leq 0. \quad (22)$$

The proof of the feasible region can be found as follow,

*Proof:* The probability constraint of (13c) can be transformed to the deterministic constraint according to the following inference

$$\begin{aligned} & \Pr \left\{ \frac{1}{\tau_i R_i - k_i} + \frac{c_{i,e}}{f_i} \leq D_{max} \right\} \\ &= \Pr \left\{ R_i \geq \frac{1}{R_i(D_{max} - D_2)} + \frac{k_i}{\tau_i} \right\} \\ &\leq 1 - \Pr \left\{ p_i \tilde{g}_{i,j}^k \leq (I_{th} + \sigma^2) 2^{\frac{1+k_i(D_{max}-D_2)}{\tau_i(D_{max}-D_2)}} - p_i \hat{g}_{i,j}^k \right\} \\ &= 1 - \int_0^{(I_{th} + \sigma^2) 2^{\frac{1+k_i(D_{max}-D_2)}{\tau_i(D_{max}-D_2)}} - p_i \hat{g}_{i,j}^k} e^{-x} dx \geq 1 - \varepsilon_2. \end{aligned} \quad (23)$$

The inequality function (23) is equivalent to (24) as,

$$[\ln(1 - \varepsilon_2) - \hat{g}_{i,j}^k] e^{\tilde{p}_i} + D^* \leq 0, \quad (24)$$

where  $D^* = (I_{th} + \sigma^2) 2^{\frac{1+k_i(D_{max}-D_2)}{\tau_i(D_{max}-D_2)}}$ . ■

Therefore, transform the deterministic optimization problem of robust power control given by equation (25), we can reformulate the objective function, outage probability constraints, and delay constraints as follows:

$$\mathbf{P1} : \max_{\mathbf{p}} \frac{1}{\ln 2} \sum_{i=1}^M \frac{U_{i,exe}}{d_{i,up}} \left[ A_k \ln(\gamma(e^{\tilde{p}})) + B_k \right] \quad (25a)$$

$$s.t. \begin{cases} \sum_{i=1}^M \chi_{i,j} e^{\tilde{p}_i} + \Pi_i \leq 0, \\ [\ln(1 - \varepsilon_2) - \hat{g}_{i,j}^k] e^{\tilde{p}_i} + D^* \leq 0, \\ -\infty \leq \tilde{p}_i \leq \ln p_{i,max}. \end{cases} \quad (25b)$$

$$(25c)$$

$$(25d)$$

### C. Optimal Power Control Algorithm

To solve the problem (25), an iterative algorithm, the Lagrange method is used to maximize the lower-bound of the original objective when two coefficients,  $X_i$  and  $Y_i$  are given. These two coefficients are updated to guarantee a monotonic increase in the lower-bound performance.

Hence, the Lagrangian function of (25) with fixed coefficients  $X_i$  and  $Y_i$  is formulated as,

$$\begin{aligned} L(\tilde{\mathbf{p}}, \lambda, \mu) &= \frac{1}{\ln 2} \sum_{i=1}^M \frac{U_{i,exe}}{d_{i,up}} \left[ A_k \ln(\gamma_k(e^{\tilde{p}})) + B_k \right] \\ &\quad - \mu_k \left[ (\ln(1 - \varepsilon_2) - \hat{g}_{i,j}^k) e^{\tilde{p}_i} + D^* \right] \\ &\quad - \lambda_k \left[ \sum_{i=1}^M \chi_{i,j} e^{\tilde{p}_i} + \Pi_i \right], \end{aligned} \quad (26)$$

where  $\lambda_k$  and  $\mu_k$  are the Lagrangian multipliers with  $\lambda_k \geq 0$  and  $\mu_k \geq 0$ .

The differential equation (27) is used to solve the power vector  $\mathbf{p}$  of the iteration function.

$$\begin{aligned} \frac{\partial L(\mathbf{p}, \lambda, \mu)}{\partial p_i} &= A_i - \left[ \sum_{j=1, j \neq i}^M \left( A_j \frac{\tilde{\gamma}_j(e^{\tilde{p}}) \bar{G}_{k,j}}{e^{\tilde{p}_j} \bar{G}_{j,j}} \right) \right. \\ &\quad \left. + \lambda_i \Pi_i e^{-\tilde{p}_i} + \mu_i \hat{g}_{i,j}^k \right] e^{\tilde{p}_i} = 0, \end{aligned} \quad (27)$$

Based on (27), the power allocation is updated iteratively by,

$$\begin{aligned} \tilde{p}^{(t+1)} &= \left[ \ln A_i + \ln \left( \sum_{j=1, j \neq i}^M \left( A_j \frac{\tilde{\gamma}_j(e^{\tilde{p}}) \bar{G}_{k,j}}{e^{\tilde{p}_j} \bar{G}_{j,j}} \right) \right. \right. \\ &\quad \left. \left. + \lambda_i \Pi_i e^{-\tilde{p}_i} + \mu_i \hat{g}_{i,j}^k \right) \right]_{-\infty}^{\ln p_{max}}, \end{aligned} \quad (28)$$

We can update the Lagrangian multipliers  $\lambda$  and  $\mu$  using the sub-gradient method, which is given as follows:

$$\lambda_i^{(t+1)} = \left[ \lambda_i^{(t)} + K_\lambda^{(t)} \left( \sum_{j \neq i}^M \chi_{i,j} e^{\tilde{p}_j} + \Pi_i \right) \right]^+, \quad (29)$$

$$\mu_{i,j}^{(t+1)} = \left[ \mu_{i,j}^{(t)} + K_\mu \left( (\ln(1 - \varepsilon_2) - \hat{g}_{i,j}^k) e^{\tilde{p}_i} + D^* \right) \right]^+, \quad (30)$$

where  $K_\lambda$  and  $K_\mu$  represent the step size for the Lagrangian multipliers,  $K_\lambda \geq 0$  and  $K_\mu \geq 0$ . The variable  $t$  is the iteration index and the positive part of the variable  $x$  is defined as  $[x]^+ = \max[0, x]$ .

### D. Computing Resource Allocation

After obtaining the optimal vector  $\mathbf{p}$ , the problem with respect vector  $\mathbf{f}$  is reformulated as:

$$\mathbf{P2} : \max_{\mathbf{f}} \sum_{i=1}^N \frac{U_{i,exe}}{t_{i,up}} \quad (31a)$$

$$s.t. \begin{cases} \Pr \left\{ \frac{1}{\tau_i R_i - k_i} + \frac{c_{i,e}}{\bar{f} + f_i} \leq D_{max} \right\} \geq 1 - \varepsilon_2, \\ \sum_{i=1}^N f_i \leq f_{total}. \end{cases} \quad (31b)$$

$$(31c)$$

Notice that the constraints in (31b) and (31c) are convex. By using the second-order derivatives of  $f_i$ , the Lagrangian function is adopted to determine the optimal computational resource. Hence, the Lagrangian function of (31) is formulated as,

$$\begin{aligned} Q(\mathbf{f}, \xi, \varphi) &= \frac{1}{\ln 2} \sum_{i=1}^M \frac{R_i(P)}{d_{i,up}} \left[ 1 - \left( \frac{c_{i,e}}{t_{max}(\bar{f} + f_i)} \right) \right. \\ &\quad \left. + \frac{T_c}{t_{max}} \right] - \xi_k \left( \frac{1}{\tau_i R_i - \lambda_i} + \frac{c_{i,e}}{\bar{f} + f_i} - D_{max} \right) \\ &\quad - \varphi_k \left[ \sum_{i=1}^M f_i - f_{total} \right]. \end{aligned} \quad (32)$$

To prove the concavity of (31a), the first-order derivative of  $Q(\mathbf{f}, \xi, \varphi)$  with respect to  $f_i$  is considered,

$$\frac{\partial Q(\mathbf{f}, \xi, \varphi)}{\partial f_i} = \frac{c_{i,e}}{\ln 2 d_{i,up} t_{max} (\bar{f} + f_i)^2} = \frac{\Omega_i}{(\bar{f} + f_i)^2}, \quad (33)$$

where  $\Omega_i = \frac{c_{i,e}}{\ln 2 d_{i,up} t_{max}}$ , the second-order derivative is,

$$\frac{\partial^2 Q}{\partial f_i^2} = -\frac{2 \cdot \Omega_i}{(\bar{f} + f_i)^3} \leq 0, \quad (34)$$

where the second-order derivative of  $Q(\mathbf{f}, \xi, \varphi)$  with respect to  $f_i$  is always less than zero. Therefore,  $Q(\mathbf{f}, \xi, \varphi)$  is a

concave function with respect to  $f_i$ . Hence, (31a) is a convex optimization problem and can be solved using Karush-Kuhn-Tucker conditions.

$$\frac{\partial (\mathbf{f}, \xi, \varphi)}{\partial f_i} = \frac{\Omega_i R_i(P)}{(\bar{f} + f_i)^2} - \xi_k \frac{c_{i,e}}{(\bar{f} + f_i)^2} - \sum_{k=1}^N \varphi_k = 0. \quad (35)$$

Let

$$\frac{\partial (\mathbf{f}, \xi, \varphi)}{\partial f_i} = 0,$$

the optimal computing resource allocation is,

$$f_i^* = \sqrt{\frac{\Omega_y R_i(P) - c_{i,e} \xi_k}{\sum_{k=1}^N \varphi_k}} - \bar{f}. \quad (36)$$

Based on (36), the optimal computing rate allocation at the  $(t+1)$ th iteration is,

$$\tilde{f}^{(t+1)} = \left[ \sqrt{\frac{\Omega_y R_i(P) - c_{i,e} \xi_k}{\sum_{k=1}^M \varphi_k}} - \bar{f} \right]_0^{f_{total}}. \quad (37)$$

The Lagrangian multiplier  $\eta$  at the  $(t+1)$ th iteration,  $\xi_i^{(t+1)}$  and  $\varphi_{i,j}^{(t+1)}$ , are updated by the sub-gradient method as,

$$\xi_i^{(t+1)} = \left[ \xi_i^{(t)} + K_\xi^{(t)} \left( \frac{1}{\tau_i R_i - \lambda_i} + \frac{c_{i,e}}{\bar{f} + f_i} - D_{max} \right) \right]^+, \quad (38)$$

$$\varphi_{i,j}^{(t+1)} = \left[ \varphi_{i,j}^{(t)} + K_\varphi \left( \sum_{i=1}^M f_i - f_{total} \right) \right]^+. \quad (39)$$

After transformed the original problem into two convex subproblems, an alternative iterative algorithm which is summarized in Algorithm 1 is proposed to solve the two convex subproblems.

---

**Algorithm 1** Robust Power Control Task Offloading Scheduling Algorithm

---

- 1: **Input:** Set the maximum number of iterations  $T_{max}$ , and the iterative index  $t = 0$ .
  - 2: **repeat**
  - 3:   Initialize the feasible points  $\lambda, \mu$  and  $\mathbf{f}$ .
  - 4:   Solve problem **P1**, and determine the current optimal solution  $\tilde{\mathbf{p}}^{(t+1)}$ .
  - 5:   Initialize the feasible points  $\xi, \varphi$  and  $\mathbf{p}$ .
  - 6:   Solve the problem **P2**, and determine the current optimal solution  $\tilde{\mathbf{f}}^{(t+1)}$ .
  - 7: **until** algorithm converges synchronously to the optimal result or  $t \geq T_{max}$ .
  - 8: **Output:**  $\mathbf{f}, \mathbf{p}$ .
- 

**Remark 2.** The time complexity of Algorithm 1 is determined by the maximal loop count,  $T_{max}$ , in its repeat-until loop. As Algorithm 1 involves  $V$  clusters performing power iterations for power optimization, its computational complexity is  $O(VT_{max})$ .

#### IV. SIMULATION RESULTS AND PERFORMANCE ANALYSIS

The performance of Algorithm 1 is evaluated through numerical simulations in this section. We consider a MEC-based vehicular network system composed of five clusters in a given time slot as our fundamental simulation scenario. The main system parameters are listed in Table II. The bandwidth  $W$  is set as 10 MHz in the numerical simulations. The system assumes that both the vehicles and RSUs use only one antenna for transmission and reception. Additionally, we assume that there is little to no variation in the speed of the vehicles during the reference time interval. Unless otherwise specified, the threshold parameter value of  $\gamma_{th}$  is assumed to be  $10^{-6}$ , and the outage probability thresholds are set to  $\varepsilon_1 = \varepsilon_2 = 0.1$ .

TABLE II: System parameters

| Parameter                                 | Value         |
|---|---------------|
| Radio Range ( $R_a$ )                     | 300 m         |
| Carrier frequency ( $f_c$ )               | 5.9 GHz       |
| CSI feedback period of vehicle ( $T$ )    | 1 ms          |
| Average speed of vehicle                  | 30 m/s        |
| Mean of background noise ( $\sigma^2$ )   | -30 dBm       |
| Maximum transmitter power ( $p_{i,max}$ ) | 0.05 W        |
| Pathloss model                            | $d^{-\theta}$ |
| Pathloss exponent ( $\theta$ )            | 3             |
| Log-normal shadowing standard deviation   | 10 dB         |

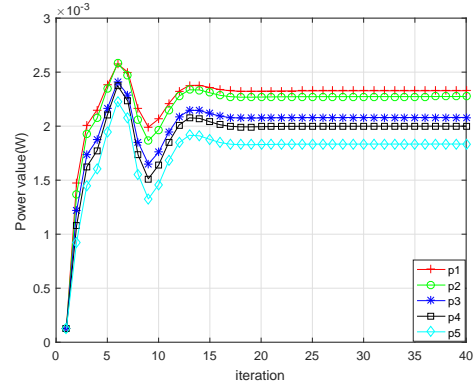


Fig. 2: Power convergence performance.

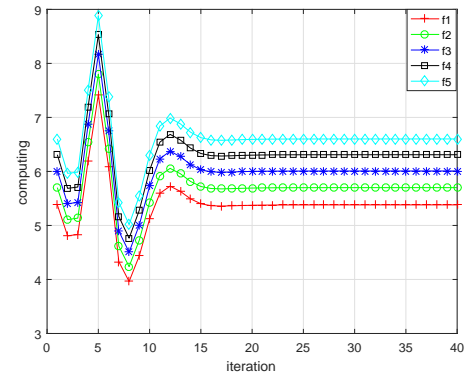


Fig. 3: Computational resource of cloud allocation to RSU.



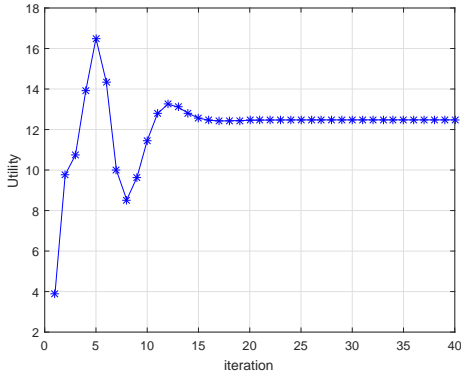


Fig. 4: Convergence of average system utility.

Fig. 2 and Fig. 3 show the power allocation of each vehicle transmitter and the corresponding computing resource of cloud allocation to RSU in Algorithm 1 respectively. The figures show the computing resources allocated in the cloud peak at the fifth iteration and begin to decline since the limitation of total computing resources  $f_{total}$  from the cloud is reached. The corresponding power resource allocation also changes due to computing resources allocation of robust power control and task offloading scheduling.

Fig. 4 shows the convergence of the total utility of the system when the joint optimization is performed. The figure shows the convergence trend of the total utility of the network system is related to power allocation and computing rate allocation. It is reasonable to observe this phenomenon because of the definition of  $U$  as given in equation (11).  $R_i$  increases logarithmically as the power vector  $\mathbf{p}$  increases, resulting in diminishing marginal gains. Therefore, as the number of iterations increases, the incremental increase in utility value becomes smaller and smaller, eventually leading to a plateau in utility value. The upload time  $t_{i,up}$ , the denominator of  $U$  decrease, when the power vector  $\mathbf{p}$  and as the executive utility of the numerator part,  $t_{i,exe}$  decreases inversely proportional with the increase of computing power vector  $\mathbf{f}$ , the numerator increases with the increase of vector  $\mathbf{f}$ .

In the MEC-Enabled vehicular cloud system, it is necessary to take into account the vehicle mobility. Next, we explored how the movement of vehicles affects system performance. We assumed that any changes in vehicle speed during the designated time period are insignificant. In order to further clarify the influence of speed-induced Doppler shift on system performance, the comparison between the benchmark value and the increasing speed measurement is simulated under the condition of constant vehicle speed in the system.

Fig. 5 demonstrates the effect of different speeds on system performance under high mobility vehicular environment. Since the relative speed in the V2R link is zero and the speed of all vehicles in the same network, there is no Doppler effect. The vehicle speed during the communication is set to 20 m/s, 30 m/s, 40 m/s, 50 m/s and 60 m/s, As depicted in Figure 5, the utility value of the vehicular network experiences a decline as the speed of the vehicle increases. Since a higher speed causes an increased Doppler frequency shift within the network, which in turn results in greater channel uncertainty

and a subsequent decrease in utility value.

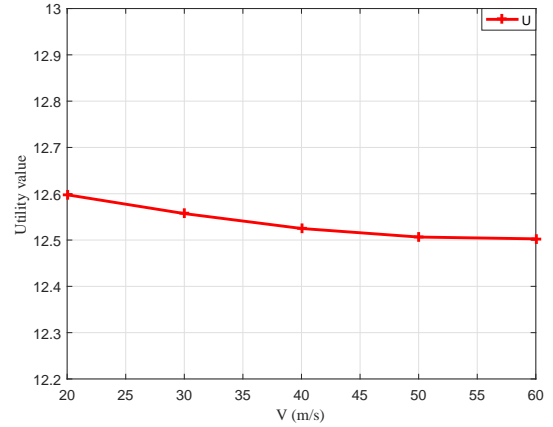


Fig. 5: Comparison of average system utilities with different speeds.

After the vehicle mobility is considered, the performance of the proposed scheme is further verified. Fig. 6 shows the effect of the same speeds and different speeds of each vehicle when different  $\varepsilon_1$  is used on the total utility. The figure shows that the system utility changes when  $\varepsilon_1$  changes. The utility at different speeds of each vehicle is higher than that of all vehicles at the same speed. This result characterizes the high robustness of the proposed method when implementing in complex dynamic vehicle networks.

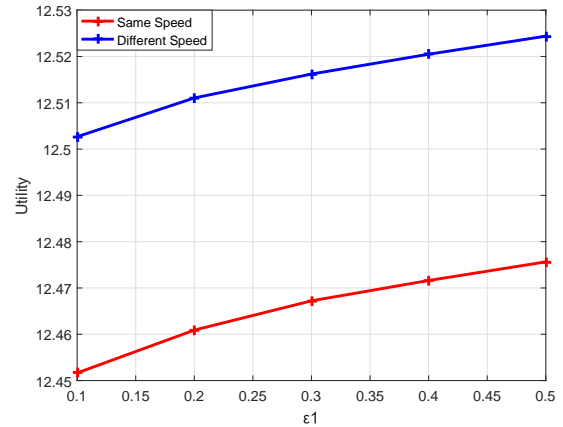


Fig. 6: Comparison of average system utility with different  $\varepsilon_1$ .

For the computing rate allocation, we choose the default task input size as  $d_u = 420KB$  (which can be referred to [28]), We evaluate the system utility performance with different benchmark schemes. It attempts to show the convergence performance of our proposed algorithm. Simulation results attempt to show that the proposed method is better than the three benchmark schemes. The benchmark schemes are described as follow

- 1) “Independently offloading and power control” (denoted as “IOP”), the vehicles independently perform power control



and computing rate allocation without the optimal value for each other.

- 2) “Without vehicle power control”(denoted as “Without-VPC”), the transmit power of the vehicles is set as the average power during the offloading.
- 3) “Without computing rate allocation” (denoted as “Without-CRA”), the computing rate allocation of the cloud is set as a fixed value during the offloading.

Fig. 7 show the iterative convergence of the total utility of the system in different cases, and the figure that shows the robust joint optimization performance is better than the other three schemes. The figure show that the four methods converge to a stable value in the late iteration and the performance of proposed scheme is the best.

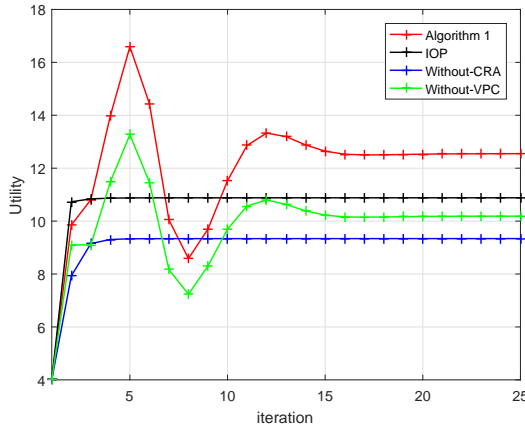


Fig. 7: System utility convergence for different methods.

In order to reflect a more realistic situation, the CPU task load (Megacycles) required for each vehicle are often different, therefore we set the CPU task load (Megacycles) of the five vehicles to 1600, 1700, 1800, 1900 and 2000. As we can see, with the increase of the iteration number, the average system utility of vehicles changes gradually and tends to be stable. In the independent optimization process, the computational rate allocation is performed first, and the optimal power allocation is not known at this time. The power and computing rate alternate optimization method is used, and the corresponding optimal value can be obtained for each iteration. Individual optimization first optimizes the power vector  $\mathbf{p}$ . After the result is obtained, the result is used to optimize of computational rate allocation, and then the computing rate are optimized, the system is obtained. However, if joint optimization is used, then both variables can achieve the optimal value if the joint optimization is used.

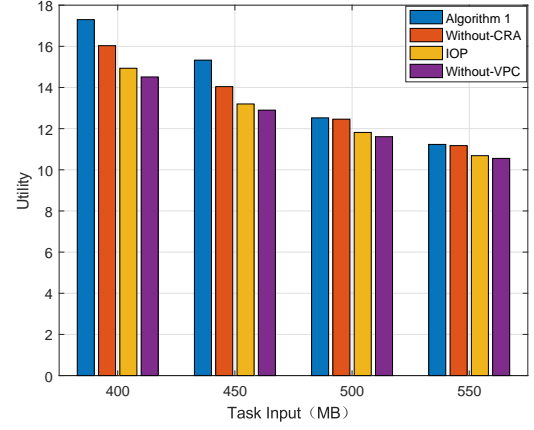


Fig. 8: Comparison of average system utility with different task input sizes  $d_u$ .

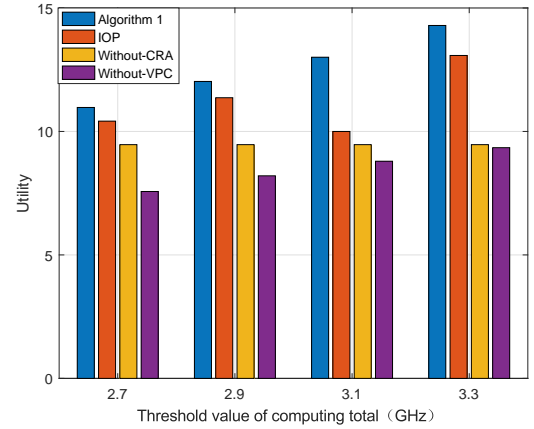


Fig. 9: Comparison of average system utility with different  $f_{total}$ .

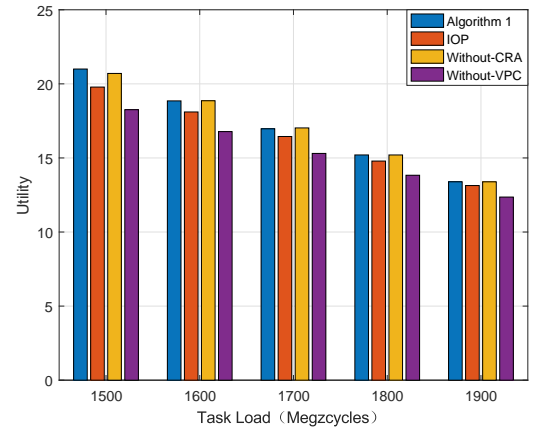


Fig. 10: Comparison of average system utility with different task workloads  $c_{i,e}$ .

The average system utility of the four competing schemes are plotted in Fig. 8 with different task input sizes  $d_u$ . The figure shows that the average system utilities of all schemes

decrease with the task input sizes increase. The figure also shows that the performance gains of the other schemes also have the similar trend. This phenomenon is reasonable, since the definition of  $U$  in (11) shows that the increase in workload has a negative impact to the system performance. Fig. 9 shows the total system cost comparisons with different  $f_{total}$ . The system utility is small when the computation capability is small, since the computational capability at the cloud is limited. We can clearly see in Fig. 10 the system utility is small when the data size increases. The computational tasks require more upload time when the data sizes are larger.

## V. CONCLUSIONS

In this paper, we have investigated a novel approach to the robust power control and task offloading for cloud assisted MEC in vehicular networks. The optimization scheme aims to guarantee vehicles' QoS is maintained when maximizing utility. Since the channel uncertainty exists, the optimization is constrained by transmission rate, computational communication latency, and probability forms of the co-channel interference. The original optimization problem was formulated as a robust power control and task offloading scheduling problem, which is very difficult to be solved. Here the SCA technique was applied to transform the NP-hard problem of variables coupling into a treatable convex problem. The robust power control and task offloading scheduling algorithm is used to develop feasible solutions. Simulation results showed that our proposed algorithm obtain the solutions which are approximate the optima. Significant improvement in terms of average system offloading utilities can be achieved, compared to the existing approaches.

## REFERENCES

- [1] X.-Q. Pham, T.-D. Nguyen, V. Nguyen, and E.-N. Huh, "Joint Node Selection and Resource Allocation for Task Offloading in Scalable Vehicle-Assisted Multi-Access Edge Computing," *Symmetry*, vol. 11, no. 1, p. 58, 2019.
- [2] R. Singh, R. Sukapuram, and S. Chakraborty, "A survey of mobility-aware Multi-access Edge Computing: Challenges, use cases and future directions," *Ad Hoc Networks*, vol. 140, p. 103044, 2023.
- [3] Y. Wang, P. Lang, D. Tian, J. Zhou, X. Duan, Y. Cao, and D. Zhao, "A Game-Based Computation Offloading Method in Vehicular Multiaccess Edge Computing Networks," *IEEE Internet of Things Journal*, vol. 7, no. 6, pp. 4987–4996, 2020.
- [4] S. Pang, N. Wang, M. Wang, S. Qiao, X. Zhai, and N. N. Xiong, "A Smart Network Resource Management System for High Mobility Edge Computing in 5G Internet of Vehicles," *IEEE Transactions on Network Science and Engineering*, vol. 8, no. 4, pp. 3179–3191, 2021.
- [5] Z. Zhou, J. Feng, Z. Chang, and X. Shen, "Energy-efficient edge computing service provisioning for vehicular networks: A consensus admm approach," *IEEE Transactions on Vehicular Technology*, vol. 68, no. 5, pp. 5087–5096, 2019.
- [6] P. Dai, K. Hu, X. Wu, H. Xing, F. Teng, and Z. Yu, "A Probabilistic Approach for Cooperative Computation Offloading in MEC-Assisted Vehicular Networks," *IEEE Transactions on Intelligent Transportation Systems*, vol. 23, no. 2, pp. 899–911, 2022.
- [7] L. T. Tan and R. Q. Hu, "Mobility-Aware Edge Caching and Computing in Vehicle Networks: A Deep Reinforcement Learning," *IEEE Transactions on Vehicular Technology*, vol. 67, no. 11, pp. 10 190–10 203, 2018.
- [8] J. Wang, K. Zhu, B. Chen, and Z. Han, "Distributed clustering-based cooperative vehicular edge computing for real-time offloading requests," *IEEE Transactions on Vehicular Technology*, vol. 71, no. 1, pp. 653–669, 2022.
- [9] Z. Li, C. Yang, X. Huang, W. Zeng, and S. Xie, "Coor: Collaborative task offloading and service caching replacement for vehicular edge computing networks," *IEEE Transactions on Vehicular Technology*, 01 2023.
- [10] A. Nemirovski and A. Shapiro, "Convex Approximations of Chance Constrained Programs," *SIAM Journal on Optimization*, vol. 17, no. 4, pp. 969–996, 2007.
- [11] Z. Liu, Y. Xie, K. Y. Chan, K. Ma, and X. Guan, "Chance-Constrained Optimization in D2D-Based Vehicular Communication Network," *IEEE Transactions on Vehicular Technology*, vol. 68, no. 5, pp. 5045–5058, 2019.
- [12] X. Li, L. Ma, Y. Xu, and R. Shankaran, "Resource Allocation for D2D-Based V2X Communication With Imperfect CSI," *IEEE Internet of Things Journal*, vol. 7, no. 4, pp. 3545–3558, 2020.
- [13] Y.-a. Xie, Z. Liu, K. Y. Chan, and X. Guan, "Energy-Spectral Efficiency Optimization in Vehicular Communications: Joint Clustering and Pricing-Based Robust Power Control Approach," *IEEE Transactions on Vehicular Technology*, vol. 69, no. 11, pp. 13 673–13 685, 2020.
- [14] H. Zhou, W. Xu, Y. Bi, J. Chen, Q. Yu, and X. S. Shen, "Toward 5G Spectrum Sharing for Immersive-Experience-Driven Vehicular Communications," *IEEE Wireless Communications*, vol. 24, no. 6, pp. 30–37, 2017.
- [15] T. X. Tran and D. Pompili, "Joint Task Offloading and Resource Allocation for Multi-Server Mobile-Edge Computing Networks," *IEEE Transactions on Vehicular Technology*, vol. 68, no. 1, pp. 856–868, 2019.
- [16] Z. Liu, C. Liang, Y. Yuan, K. Y. Chan, and X. Guan, "Resource Allocation Based on User Pairing and Subcarrier Matching for Downlink Non-Orthogonal Multiple Access Networks," *IEEE/CAA Journal of Automatica Sinica*, vol. 8, no. 3, pp. 679–689, 2021.
- [17] S. Wang, W. Shi, and C. Wang, "Energy-Efficient Resource Management in OFDM-Based Cognitive Radio Networks Under Channel Uncertainty," *IEEE Transactions on Communications*, vol. 63, no. 9, pp. 3092–3102, 2015.
- [18] H. Xiao, D. Zhu, and A. T. Chronopoulos, "Power Allocation With Energy Efficiency Optimization in Cellular D2D-Based V2X Communication Network," *IEEE Transactions on Intelligent Transportation Systems*, vol. 21, no. 12, pp. 4947–4957, 2020.
- [19] Y. Chen, Y. Wang, and L. Jiao, "Robust Transmission for Reconfigurable Intelligent Surface Aided Millimeter Wave Vehicular Communications With Statistical CSI," *IEEE Transactions on Wireless Communications*, vol. 21, no. 2, pp. 928–944, 2022.
- [20] T. Kim, D. J. Love, and B. Clerckx, "Does Frequent Low Resolution Feedback Outperform Infrequent High Resolution Feedback for Multiple Antenna Beamforming Systems?" *IEEE Transactions on Signal Processing*, vol. 59, no. 4, pp. 1654–1669, 2011.
- [21] A. Sakr and E. Hossain, "Cognitive and Energy Harvesting-Based D2D Communication in cellular networks: Stochastic geometry modeling and analysis," *IEEE Transactions on Communications*, vol. 63, pp. 1867–1880, 05 2014.
- [22] C. Guo, L. Liang, and G. Y. Li, "Resource allocation for high-reliability low-latency vehicular communications with packet retransmission," *IEEE Transactions on Vehicular Technology*, vol. 68, no. 7, pp. 6219–6230, 2019.
- [23] K. Zhang, Y. Mao, S. Leng, Y. He, and Y. ZHANG, "Mobile-Edge Computing for Vehicular Networks: A Promising Network Paradigm with Predictive Off-Loading," *IEEE Vehicular Technology Magazine*, vol. 12, no. 2, pp. 36–44, 2017.
- [24] U. Saleem, Y. Liu, S. Jangsher, Y. Li, and T. Jiang, "Mobility-aware joint task scheduling and resource allocation for cooperative mobile edge computing," *IEEE Transactions on Wireless Communications*, vol. 20, no. 1, pp. 360–374, 2021.
- [25] S. Liu, J. Tian, X. Deng, Y. Zhi, and J. Bian, "Stackelberg game-based task offloading in vehicular edge computing networks," *International Journal of Communication Systems*, vol. 34, no. 16, p. e4947, 2021.
- [26] Z. Liu, J. Su, Y.-a. Xie, K. Ma, Y. Yang, and X. Guan, "Resource Allocation in D2D-Enabled Vehicular Communications: A Robust Stackelberg Game Approach Based on Price-Penalty Mechanism," *IEEE Transactions on Vehicular Technology*, vol. 70, no. 8, pp. 8186–8200, 2021.
- [27] D. P. Bertsekas, "Nonlinear Programming: 2nd Edition," 1999.
- [28] X. Chen, L. Jiao, W. Li, and X. Fu, "Efficient multi-user computation offloading for mobile-edge cloud computing," *IEEE/ACM Transactions on Networking*, vol. 24, no. 5, pp. 2795–2808, 2016.